Substantial restoration of night vision in adult mice with congenital stationary night blindness

Juliette Varin,[1] Nassima Bouzidi,[1] Gregory Gauvain,[1,7] Corentin Joffrois,[1,7] Melissa Desrosiers,[1] Camille Robert,[1] Miguel Miranda De Sousa Dias,[1] Marion Neuillé,[1] Christelle Michiels,[1] Marco Nassisi,[1] José-Alain Sahel,[1,2,3,4,5] Serge Picaud,[1] Isabelle Audo,[1,2,6] Deniz Dalkara,[1] and Christina Zeitz[1]

[1]Sorbonne Université, INSERM, CNRS, Institut de la Vision, Paris, France; [2]Centre Hospitalier National d'Ophtalmologie des Quinze-Vingts, INSERM-DHOS CIC 1423, Paris, France; [3]Fondation Ophtalmologique Adolphe de Rothschild, Paris, France; [4]Academie des Sciences, Institut de France, Paris, France; [5]Department of Ophthalmology, The University of Pittsburgh School of Medicine, Pittsburgh, PA 15213, USA; [6]Institute of Ophthalmology, University College of London, London, UK

Complete congenital stationary night blindness (cCSNB) due to mutations in *TRPM1, GRM6, GPR179, NYX*, or leucine-rich repeat immunoglobulin-like transmembrane domain 3 (*LRIT3*) is an incurable inherited retinal disorder characterized by an ON-bipolar cell (ON-BC) defect. Since the disease is non-degenerative and stable, treatment could theoretically be administrated at any time in life, making it a promising target for gene therapy. Until now, adeno-associated virus (AAV)-mediated therapies lead to significant functional improvements only in newborn cCSNB mice. Here we aimed to restore protein localization and function in adult *Lrit3*$^{-/-}$ mice. LRIT3 localizes in the outer plexiform layer and is crucial for TRPM1 localization at the dendritic tips of ON-BCs and the electroretinogram (ERG)-b-wave. AAV2-7m8-*Lrit3* intravitreal injections were performed targeting either ON-BCs, photoreceptors (PRs), or both. Protein localization of LRIT3 and TRPM1 at the rod-to-rod BC synapse, functional rescue of scotopic responses, and ON-responses detection at the ganglion cell level were achieved in a few mice when ON-BCs alone or both PRs and ON-BCs, were targeted. More importantly, a significant number of treated adult *Lrit3*$^{-/-}$ mice revealed an ERG b-wave recovery under scotopic conditions, improved optomotor responses, and on-time ON-responses at the ganglion cell level when PRs were targeted. Functional rescue was maintained for at least 4 months after treatment.

INTRODUCTION

Congenital stationary night blindness (CSNB) is a heterogeneous group of non-progressive rare inherited retinal disorders (IRDs).[2] The most frequent type of CSNB is the Schubert-Bornschein-type, which is due to a disruption of the signal transmission between photoreceptors (PRs) and ON-bipolar cells (ON-BCs).[1,2] CSNB can be further subdivided into the incomplete CSNB (icCSNB) and complete CSNB (cCSNB) forms.[3] Here we focus on the latter one. cCSNB-affected subjects are mainly characterized by impairment of night vision, decreased visual acuity, severe myopia, nystagmus, and sometimes strabismus. cCSNB is mostly a non-degenerative disease with normal fundus. Clinically, it can be diagnosed by full-field electroretinogram (ERG) recording showing an isolated ON-BC defect.[4] At low light intensities in dark-adapted (DA, scotopic) conditions, the b-wave is absent. With a brighter flash, the a-wave is normal, representing normal rod and cone function, while the b-wave remains absent in keeping with a transmission defect between PRs and ON-BCs. In light-adapted (LA, photopic) conditions, the responses to a single flash reveal a sharply arising b-wave with no oscillatory potentials and variable but often decreased b/a ratio indicating cone ON-BC dysfunction.[2] This is in accordance with the expression of the genes mutated in patients with cCSNB including *NYX*,[5,6] *TRPM1*,[7–9] *GRM6*,[10,11] *GPR179*,[12,13] and leucine-rich repeat immunoglobulin-like transmembrane domain 3 (*LRIT3*).[14] These genes code for proteins localized in the outer plexiform layer (OPL) affecting signal transmission between PRs and ON-BCs.[2] Several mouse models of cCSNB have been described. All display an absence of ERG b-wave under both scotopic and photopic conditions.[2,15] While the scotopic phenotype is similar to those of patients, the b-wave under photopic conditions is only reduced in patients. Herein, we focus on cCSNB due to mutations in LRIT3 coding for the LRIT3 protein using the respective mouse model (*nob6* also called *Lrit3*$^{-/-}$).[14,16] *Lrit3*$^{-/-}$ mice are characterized by the absence of LRIT3 in the OPL, a lack of the ERG b-wave under both scotopic and photopic conditions, altered optomotor responses under scotopic conditions, and abolished ON-responses at the RGC level.[16,17] The outer nuclear layer (ONL) is generally well preserved.[16] Only some disorganized synaptic contacts of ON-BC at the cone pedicle but not at the rod spherule without ultrastructural alterations in cone terminals, horizontal cells, or synaptic ribbons were described.[17] LRIT3 is crucial for the correct localization of TRPM1 at the dendritic tips of all ON-BCs, cone synapse formation, and/or maintenance[18] and is essential for the localization of nyctalopin, encoded by *NYX*.[19] Several gene therapies for IRDs have been developed over the years.[20] However, treatment for CSNB patients is yet unavailable and gene replacement therapy might
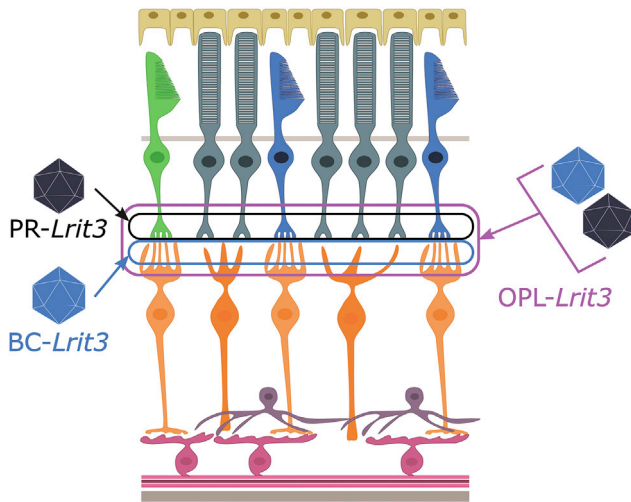
Figure 1. Schematic representation of the cellular targets of the three constructs

PR-*Lrit3* construct targeting both rod (gray) and cone (blue, green) PRs, the BC-*Lrit3* construct targeting both rod (dark orange) and cone ON-BCs (light orange), and the OPL-*Lrit3* construct targeting both rod and cone PRs and ON-BCs by co-injection of the PR-*Lrit3* and BC-*Lrit3* constructs.

be the most promising approach to treat this disorder. cCSNB represents a non-progressive disorder, in which retinal morphology is well preserved.[18] Genes underlying this disorder have been identified and specific targeting of ON-bipolar cells in primate retinas with adeno-associated virus (AAV)-vectors has been demonstrated.[21] Due to this stable non-degenerative condition in mice and human, treatment could be, in theory, administrated at any time during the course of life. However, recent findings revealed functional restoration mainly in very young mice.[22,23] In mice lacking *Nyx* and treated at 2 days of age (P2) with targeting only the ON-BCs, partial functional rescue of the b-wave under scotopic conditions using an intravitreal AAV-mediated gene replacement approach has been obtained.[22] Similar observations were made in mice lacking *Lrit3*: targeting of rod PR at P5 or P35 resulted in more significant restoration at P5 compared to P35.[23] After gene therapy in adult mice lacking *Grm6*, mGluR6 and other proteins of the same cascade were localized at the dendritic tips of ON-BCs in the absence of functional restoration.[24] In addition, in all models, localization of TRPM1 at the dendritic tips of ON-BCs was observed,[22–24] while no restoration of the b-wave under photopic conditions could be obtained.[16,22,23] Here, we aimed to achieve a robust functional rescue in mature *Lrit3*^{−/−} retinas using different AAV-promoter combinations targeting ON-BCs, both rod and cone PRs, or the OPL.

RESULTS

Immunolocalization studies on unaffected patients and mouse retinas showed LRIT3 protein in the OPL, between PRs and ON-BCs.[14,18,23] It is a matter of debate whether this correlates with postsynaptic localization at the dendritic tips of ON-BCs or/and a presynaptic localization at the synapse of PRs. To revert the phenotype of *nob6* mice (later

referred as *Lrit3*^{−/−}) toward normal function, we used the following two promoter constructs: a 200 bp enhancer of *Grm6*, which has been previously shown by us to drive expression of GFP to ON-BCs,[21] and the h*GRK* promoter, which drives expression in both rod and cone PRs.[25] These two constructs were encapsidated in the AAV2-7m8 serotype[26] and injected either alone or together at a ratio of 1:1. Mice injected with the *Grm6* promoter construct will be named *Lrit3*^{−/−}-BC-*Lrit3*, mice treated with the *GRK* promoter construct will be named *Lrit3*^{−/−}-PR-*Lrit3*, and mice injected with both constructs will be named *Lrit3*^{−/−}-OPL-*Lrit3* (Figure 1).

Protein localization of LRIT3 at the rod-to-rod BC synapse

In the *Lrit3*^{−/−} mice, LRIT3 synthesis and localization is abolished in the OPL in both rod-to-rod BC and cone-to-cone ON-BC synapses[18] (Figure 2A; arrows and arrowheads, respectively). The proper localization of LRIT3 following treatment was investigated using immunolocalization studies. All treated retinas, *Lrit3*^{−/−}-BC-*Lrit3*, *Lrit3*^{−/−}-OPL-*Lrit3*, and *Lrit3*^{−/−}-PR-*Lrit3*, injected at P30, displayed LRIT3 immunostaining in the OPL, which is absent in untreated *Lrit3*^{−/−} retinas (Figure 2A; Figure S1A). In addition, *Lrit3*^{−/−} mice lack mGluR6 at the cone-to-cone ON BC synapse and TRPM1 in both rod-to-rod BC and cone-to-cone BC synapses (Figure 2). After treatment, the majority of LRIT3 staining appeared at most likely rod-to-rod BC synapses (Figure 2A, arrow), while presumably cone-to-cone BC synapse staining (Figure 2A, arrowheads) remained spared. These observations were confirmed with co-staining studies using mGluR6, a marker for both synapses; PKCα, a marker of rod BCs; and cone arrestin or PNA, markers for the cone-to-cone BC synapse. While co-staining of LRIT3 with mGluR6 at the rod-to-rod BC is present (Figure 2A, arrows; Figure S1B), LRIT3 and mGluR6 remained absent at the cone-to-cone BC synapse in treated retinas (Figures 2A and 2B; Figure S1B). Thinning or remodeling of the ONL in the *Lrit3*^{−/−} or treated mice was absent.

Treatment results in TRPM1 localization at the dendritic tips of rod BCs

To ensure correct ON-BC signal transmission, the correct localization of TRPM1 at the dendritic tips of ON-BCs is essential. In the *Lrit3*^{−/−} mouse model, in which TRPM1 is still present in the cell bodies of ON-BCs, the dendritic tip staining at the ON-BCs is abolished[18] (Figure 2C, TRPM1). Localization of TRPM1 following treatment that targets either PRs or ON-BCs was investigated using immunolocalization studies. In all treated retinas, TRPM1 was localized at the dendritic tips of rod BCs (Figure 2C, TRPM1). TRPM1 staining at the presumed dendritic tips of cone ON-BCs was undetectable. These results indicate that restoration of the signaling cascade was selective for the rod-to-rod BC synapse.

Positive long-lasting effect of AAV-mediated LRIT3 expression on the ERG b-wave

In *Lrit3*^{−/−} animals, the transmission of the visual signal between PRs and ON-BCs is disrupted as shown by the absence of the b-wave on the ERG under scotopic and photopic conditions[16] (Figure 3). ERG recordings performed 2 months after treatment on *Lrit3*^{−/−}-BC-*Lrit3*
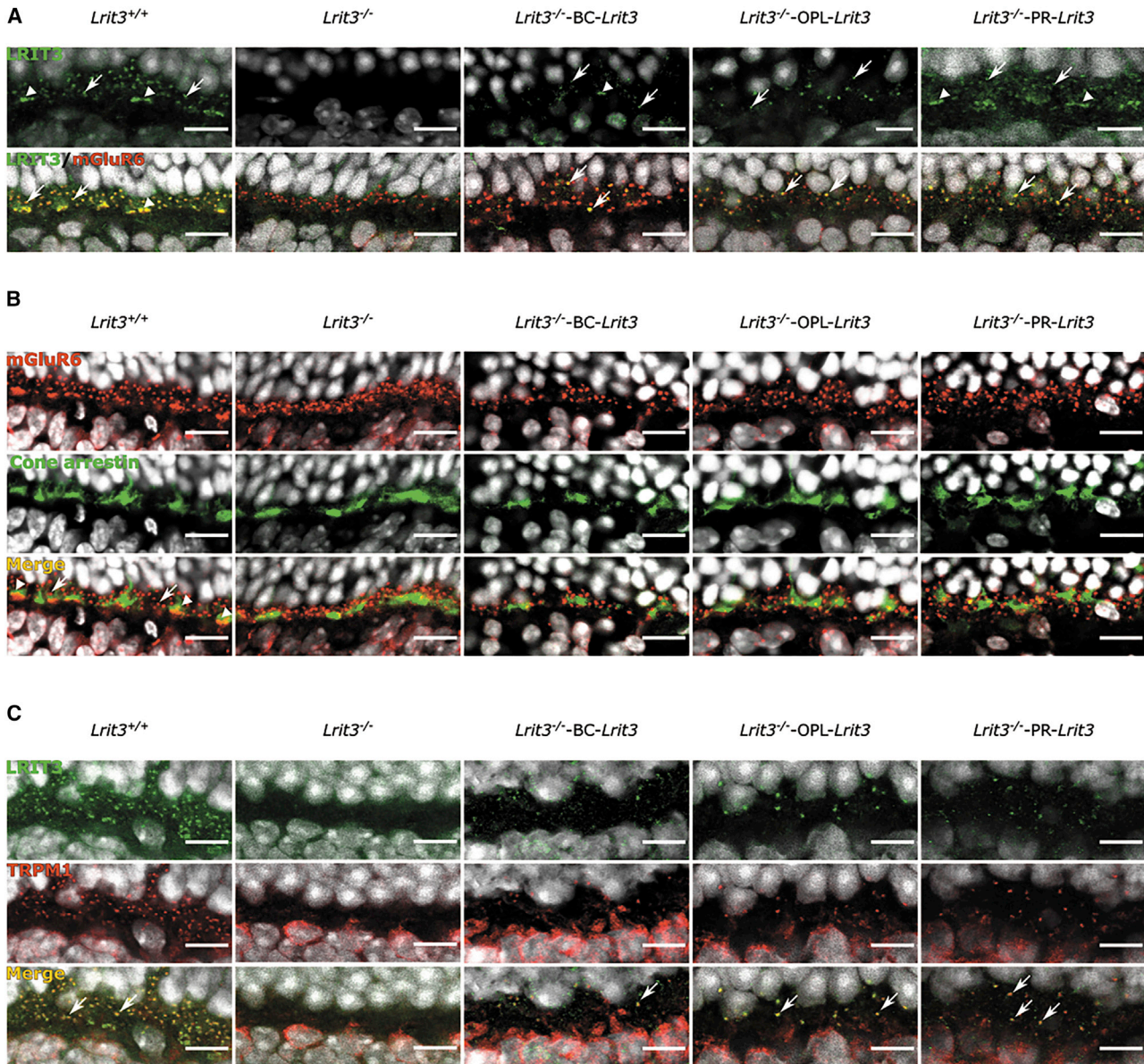
Figure 2. Localization of LRIT3 and TRPM1

Representative confocal images of cross-sections centered on the OPL of $Lrit3^{+/+}$, $Lrit3^{-/-}$, $Lrit3^{-/-}$-BC-$Lrit3$, $Lrit3^{-/-}$-OPL-$Lrit3$, and $Lrit3^{-/-}$-PR-$Lrit3$ retinas stained with an antibody against (A) LRIT3 (green) and mGluR6 (red); (B) mGluR6 (red) and cone-arrestin (green); and (C) LRIT3 (green) and TRPM1 (red). Arrows indicative putative rod-to-rod BC and arrow heads putative cone-to-cone ON-BC synapses. Scale bars, 10 μm.

mice injected at P30 revealed a partial b-wave under scotopic conditions, while the photopic b-wave was absent (Figures 3A, left, and 3B). Highest restoration was found at the lowest flash intensity. The amplitude of the b-wave corresponded to 45% compared to the b-wave amplitudes of $Lrit3^{+/+}$ mice (Figure 3C). However, these results were obtained in a statistically non-significant number of $Lrit3^{-/-}$-BC-$Lrit3$ mice (n = 2). Similarly, ERG recordings in $Lrit3^{-/-}$-OPL-$Lrit3$ mice treated at P30 also presented a b-wave under scotopic conditions (Figure 3A, middle) corresponding to 45% of the b-wave

amplitude of $Lrit3^{+/+}$ mice at the lowest light intensity (Figure 3C). As for $Lrit3^{-/-}$-BC-$Lrit3$ mice, the scotopic b-wave was the highest at low flash intensities and the restoration was only observed under scotopic conditions (Figures 3A–3C). Only a few treated mice (n = 2) revealed this functional restoration. Strikingly, better restoration was obtained in $Lrit3^{-/-}$-PR-$Lrit3$ animals (n = 6) treated at P30 under scotopic conditions (Figure 3A, right). The amplitude of the scotopic b-wave at the flash intensity of -2.5 log cd $\times$ s/m^2 improved to 58% compared to the b-wave amplitude of $Lrit3^{+/+}$
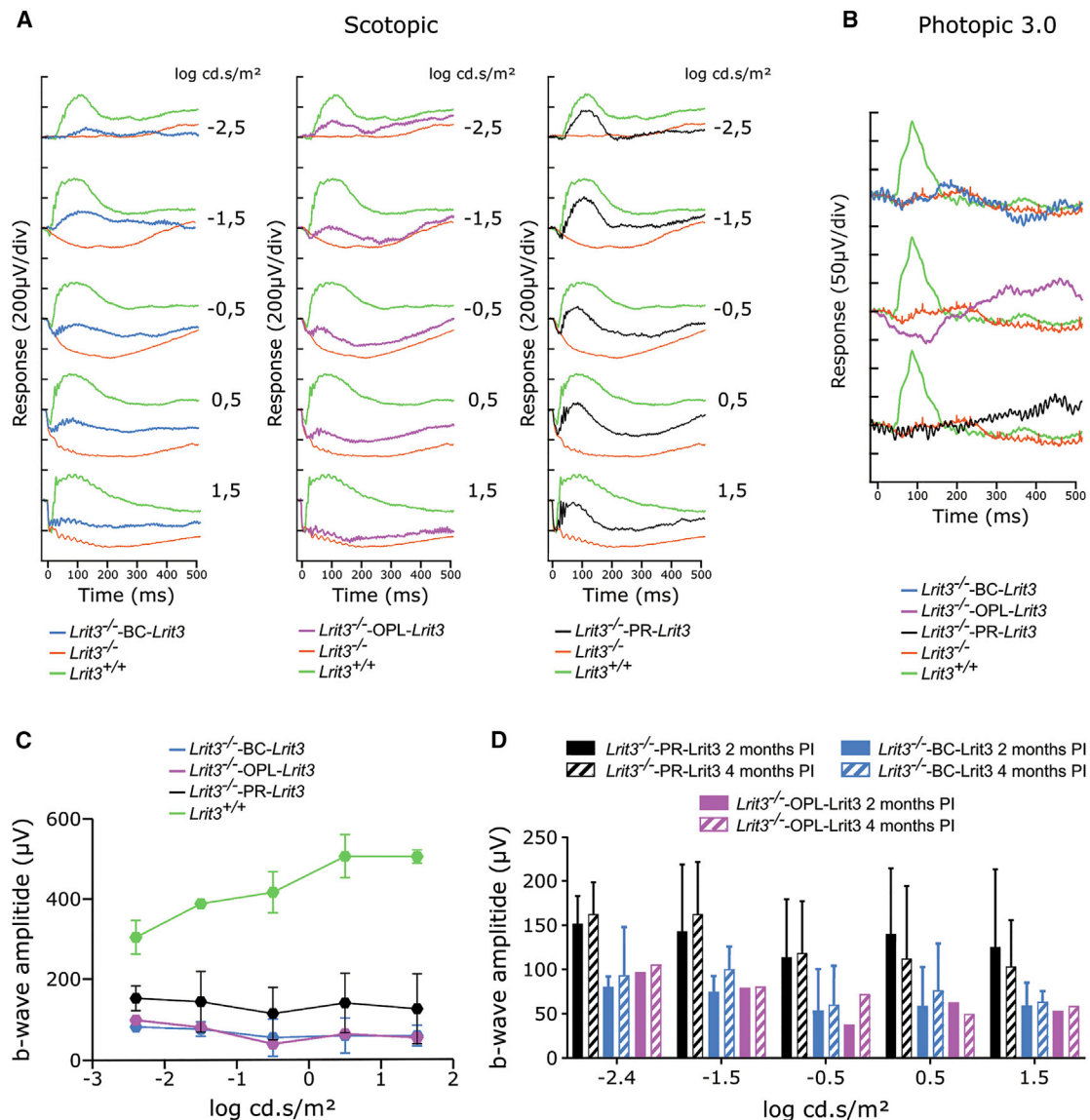
Figure 3. ERG recordings

(A) Representative scotopic ERG traces at 2 months post-injection for one $Lrit3^{+/+}$ (green line), one $Lrit3^{-/-}$ (red line), one $Lrit3^{-/-}$-BC-$Lrit3$ (blue line), one $Lrit3^{-/-}$-OPL-$Lrit3$ (purple line), and one $Lrit3^{-/-}$-PR-$Lrit3$ (black line) mice, values on the right of the row of waveforms specify the flash intensity in log cd. s/m². (B) Representative photopic ERG traces of the same mice at 2 months post-injection for a flash intensity of 3.0 cd. s/m². (C) Average amplitude of the scotopic ERG b-wave at 2 months post-injection for $Lrit3^{+/+}$ (green line, n = 5), $Lrit3^{-/-}$-BC-$Lrit3$ (blue, n = 2), $Lrit3^{-/-}$-OPL-$Lrit3$ (purple, n = 1), and $Lrit3^{-/-}$-PR-$Lrit3$ (black, n = 6) mice. (D) Comparison between the average amplitude of the scotopic ERG b-wave at 2 months (filled) and 4 months (hatched) post-injection for $Lrit3^{-/-}$-BC-$Lrit3$ (blue, n = 2), $Lrit3^{-/-}$-OPL-$Lrit3$ (purple, n = 1), and $Lrit3^{-/-}$-PR-$Lrit3$ (black, n = 5) mice revealed no statistically significant difference between 2 and 4 months for the $Lrit3^{-/-}$-PR-$Lrit3$ mice

mice (Figure 3A). To assess the duration of this partial rescue, we made a follow-up ERG recording up to 4 months post-injection. In all animals presenting a b-wave, independently of the construct used, the b-wave was still recordable and of sustained amplitude (no statistically significant change) 4 months after treatment (Figure 3D). The number of treated mice versus the number of mice presenting a scotopic b-wave for every construct is mentioned in Table 1. The functional rescue was obtained in 25% of PR-$Lrit3$ injected mice,

10% of OPL-$Lrit3$ injected mice, and ~6% of BC-$Lrit3$ injected mice (Table 1).

Presence of ON-BC signaling reveals ON-responses in RGCs in treated mice

As previously described, in $Lrit3^{-/-}$ mice ON-responses are also abolished at the level of retinal ganglion cells (RGCs)[17] (Figure 4). Correct localization of LRIT3 is mandatory for TRPM1 localization and

Table 1. Experimental data on the treatment procedure

Date of injection	Construct used	Viral preparation	Total number		Responding mice		Experimentator
			Female	Male	Female	Male	
03/06/2019			4	2	1 (71% b-wave rescue)	0	
01/11/2019			2	6	1 (49% b-wave rescue)	0	
06/12/2019	PR-Lrit3	Same	0	4	0	1 (44% b-wave rescue)	J.V.
						1 (65% b-wave rescue)	
						1 (61% b-wave rescue)	
04/01/2020			2	4	1 (56% b-wave rescue)	0	
15/11/2016		1	4	2	0	0	
27/02/2017			0	2	1 (50% b-wave rescue)	0	
10/04/2018			0	3	0	0	
11/05/2018	BC-Lrit3	2	2	4	0	0	J.D.
25/05/2018			5	0	0	0	M.S.
10/04/2018			0	3	0	0	
12/04/2019		3	2	1	0	0	J.V.
27/05/2019			1	4	0	1 (40% b-wave rescue)	
03/07/2019	OPL-Lrit3	same	5	5	0	1 (45% b-wave rescue)	

J.V., Juliette Varin; J.D., Julie Dégardin ; M.S., Manuel Simonutti

function to propagate the visual signal toward ON-ganglion cells. To confirm functional rescue following treatment, we used a 256 channel multi-electrode array (MEA-256) to record light-evoked responses in isolated retinas from $Lrit3^{+/+}$ (3 animals, 6 retina explants), $Lrit3^{-/-}$ (6 animals, 6 retina explants), $Lrit3^{-/-}$-BC-$Lrit3$ (1 animal, 1 retina explant), $Lrit3^{-/-}$-OPL-$Lrit3$ (1 animals, 1 retina explant), and $Lrit3^{-/-}$-PR-$Lrit3$ (4 animals, 4 retina explants) and assessed the potential ON-response at the level of ganglion cells. $Lrit3^{-/-}$ retina were untreated control samples, contralateral of the treated eye in the different conditions. In contrast to $Lrit3^{+/+}$ retinas, untreated $Lrit3^{-/-}$ retinas display only a few ON-responses with small spike frequency and high temporal variability (4.5 ± 3 Hz and 1.3 ± 0.6 s; Figures 4A and 4B). Furthermore, in untreated $Lrit3^{-/-}$ retinas, 33% of the light-responsive ganglion cells displayed small amplitude ON-responses (ON + ON-OFF: 37/112 responsive electrodes; Figure 4C). In comparison, RGCs from $Lrit3^{-/-}$-BC-$Lrit3$ retinas also displayed small and variable ON-responses (7.9 ± 7.5 Hz and 1 ± 0.5 s; Figures 4A and 4B). Nonetheless, a higher fraction of RGCs displayed ON-responses, with ~45% of light-sensitive ganglion cells for $Lrit3^{-/-}$-BC-$Lrit3$ (ON + ON-OFF: 34/75; Figure 4C). As expected, in $Lrit3^{-/-}$-PR-$Lrit3$ and $Lrit3^{-/-}$-OPL-$Lrit3$ retinas, peak firing rate for ON-responses were higher and closer to the stimulus onset (14.7 ± 9.5 Hz and 0.45 ± 0.4 s; 15.3 ± 12 and 0.74 ± 0.57, respectively; Figures 4A and 4B). Concerning the number of light-responsive RGCs displaying ON-responses, $Lrit3^{-/-}$-PR-$Lrit3$ but not $Lrit3^{-/-}$-OPL-$Lrit3$ retinas showed an increase in the proportion of ON-responses in the overall RGC population recorded ($Lrit3^{-/-}$-PR-$Lrit3$: ~79%, 148/187; $Lrit3^{-/-}$-OPL-$Lrit3$: ~36%, 41/113; Figure 4C). To establish whether the rescued ON-responses observed here were due to the restoration of the mGluR6 signaling, we performed experiments with bath application of the mGluR6 agonist (L-AP4) on our different conditions (Figure S2). Surprisingly, although L-AP4 blocked the ON-responses observed in $Lrit3^{-/-}$-OPL-$Lrit3$ and $Lrit3^{-/-}$-PR-$Lrit3$ retinas, with reduced firing rate and fewer electrodes recording ON-responses, it does not seem to affect the ON-responses recorded in $Lrit3^{-/-}$-BC-$Lrit3$ retinas. More retina explants of these mice would be necessary for further understanding.

Presence of LRIT3 improves optomotor responses in treated mice

It has been shown that the transmission defect between PRs and ON-BCs in the $Lrit3^{-/-}$ mouse had an impact on the visual perception of these mice.[16] Thus, treated animals with a partial functional rescue as determined by ERG recordings and MEA were subjected to measurements of optomotor responses as described before.[18,27] For the two types of treated mice, $Lrit3^{-/-}$-BC-$Lrit3$ and $Lrit3^{-/-}$-OPL-$Lrit3$, optomotor reflexes improved compared to untreated $Lrit3^{-/-}$ mice. However, the animal number for each category is low and no statistical analysis could be conducted. Strikingly, the $Lrit3^{-/-}$-PR-$Lrit3$ mice revealed a statistically significant improvement of the optomotor responses, compared to untreated $Lrit3^{-/-}$ mice (n = 8), for the two lowest spatial frequencies under scotopic conditions (n = 4, p = 0.006 for the first spatial frequency, and p = 0.03 for the second; Figure 5). Under photopic conditions, untreated $Lrit3^{-/-}$ mice presented diminished optomotor responses compared to $Lrit3^{+/+}$ mice (p = 0.001), and no statistically significant improvement of these responses were observed in $Lrit3^{-/-}$-PR-$Lrit3$ mice compared to untreated $Lrit3^{-/-}$ mice (Figure S3).
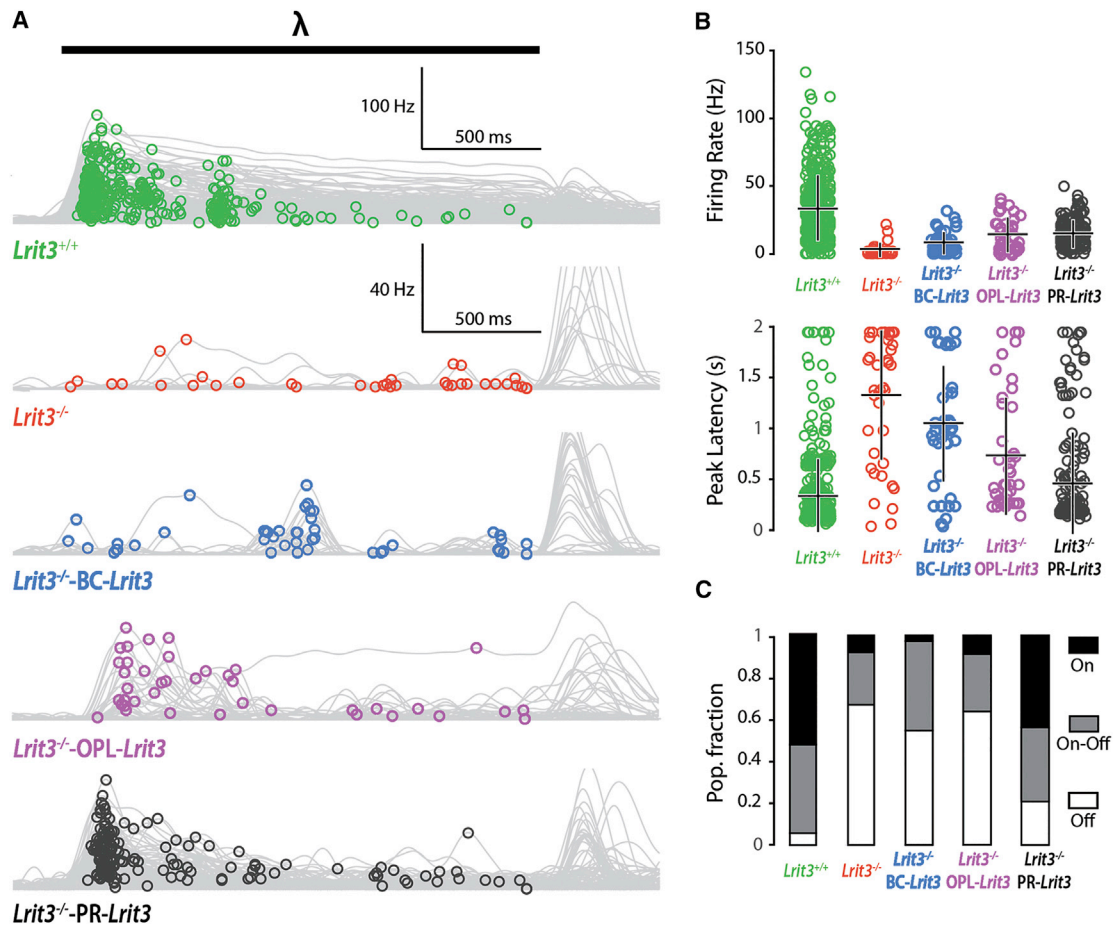
Figure 4. ON-responses in treated retinas using MEA-256 recordings

(A) Spike density function for all responsive ganglion cells displaying an ON component (ON only and ON-OFF) recorded on all treated retina (1 $Lrit3^{-/-}$-BC-$Lrit3$ [34 RGCs], 1 $Lrit3^{-/-}$-OPL-$Lrit3$ retina [41 RGCs], 4 $Lrit3^{-/-}$-PR-$Lrit3$ retina [148 RGCs], 6 $Lrit3^{-/-}$ retina [37 RGCs], and 6 $Lrit3^{+/+}$ retina [315 RGCs]). Light stimuli are indicated as a black bar (light intensity at 4.10^{11} photons/cm²/s) and light gray area, responses recorded for individual ganglion cells are displayed as gray line (average of 10 repetitions), and the peak firing rate amplitude and latency are overlaid with the traces as colored open circle. $Lrit3^{+/+}$ recording have a different scaling (upper left) than all other conditions (middle). (B) ON peak firing rate (up) and ON peak latency (bottom) for all RGCs with ON responses in the different conditions. Horizontal black bar represents the average value, and vertical black bar the mean ± SD. (C) Fraction of the recorded ganglion cells displaying ON, ON-OFF, or OFF profile of response. Surprisingly, only 5.75% ± 4% of wild-type cells displayed OFF responses. Unresponsive ganglion cells (where spontaneous activity is recorded without light-evoked spiking) are not shown here ($Lrit3^{+/+}$ = 220 cells, $Lrit3^{-/-}$ = 249 cells, $Lrit3^{-/-}$-PR-$Lrit3$ = 369 cells, $Lrit3^{-/-}$-BC-$Lrit3$ = 50 cells, and $Lrit3^{-/-}$-OPL-$Lrit3$ = 41 cells).

DISCUSSION

Over 2 million people worldwide are affected by IRDs, yet no treatment is available for most cases. An FDA approved gene therapy product (Luxturna, Sparks Therapeutics) has been available for 3 years to treat one of the most severe IRDs, Leber Congenital Amaurosis caused by mutations in *RPE65* gene. This milestone opened the way to develop additional gene therapies for other well-characterized IRDs.[28–32] Here we aimed to restore a cCSNB phenotype, another IRD, by analyzing the $Lrit3^{-/-}$ mouse model. As the name implicates, cCSNB is present since birth, does not evolve over time, and represents a signal transmission defect between PRs and ON-BCs.[2] In addition, the retinal structure is preserved, e.g., the morphology of PR and BCs are largely normal; hence, treatment should be applicable at adult ages.[2] However,

two previously reported gene therapy approaches for cCSNB described partial functional rescue mainly in newborn mice (injection at P2 or P5 versus injection at P30 or P35).[22,23] Given that, a gene therapy approach in newborn patients is less feasible than in adults, combined with the non-progressive nature of cCSNB prompted us to investigate functional restoration in the mouse model $Lrit3^{-/-}$ at the adult stage of P30. Gene therapy for cCSNB is difficult as proteins involved are part of a complex cascade and the localization and function of all of these is not clearly elucidated. However, our study shows that it is indeed achievable to obtain a strong rescue after treatment, at the protein level and at the functional level, in adult CSNB mice, most likely due to the use of a highly specific AAV capsid (AAV2.7m8), which has already been shown to efficiently transduce all retinal layers.[26]

A

B

Figure 5. Optomotor responses under scotopic conditions

(A) Histogram representation of the number of head movements recorded in 2 min, which was obtained under scotopic conditions with spatial frequencies of 0.063 and 0.125 cycles/degree for $Lrit3^{-/-}$-BC-$Lrit3$ (blue), $Lrit3^{-/-}$-OPL-$Lrit3$ (purple), and $Lrit3^{-/-}$-PR-$Lrit3$ (black) mice and compared using Mann-Whitney statistical test with representative $Lrit3^{+/+}$ (green) and $Lrit3^{-/-}$ (red) mice. The star indicates a significant test (p < 0.05). (B) Quantification of the number of head movements under scotopic and photopic conditions as presented before.[27]

Previously, LRIT3 was thought to be localized post-synaptically at the dendritic tips of ON-BCs in the OPL due to the isolated ON-BC defect observed in cCSNB patients[14] and other proteins involved in cCSNB, localizing at the ON-BCs dendritic tips.[2] Now expression data[33] and the partial restoration of function in $Lrit3$ KO mice when rods are targeted[23] suggest PR expression of $Lrit3$ and presynaptic localization. Although despite many studies, the pre- or post-synaptic localization of LRIT3 has not been clearly elucidated, it is certainly essential at the OPL in human and mouse retina.[14,18,19,23] Thus, our approach included transgene expression of LRIT3. To achieve this goal, we tested different vector-promoter combinations in $Lrit3^{-/-}$ mice. Our findings revealed partial restoration of the cCSNB phenotype when $Lrit3$ was expressed in either ON-BCs, photoreceptors, or both. Therefore, the exact $Lrit3$ expression in one or the other retinal cell type remains unresolved. In addition, even though RNA *in situ* studies were already done before showing a strong expression of $Lrit3$ in the ONL,[23] we are aware of a dog model lacking $Lrit3$, in which the function was also restored after targeting ON-BCs.[34] This latest argues in favor of an expression of $Lrit3$ in ON-BCs even though leakiness of the vectors ending up in expression of the transgene in other retinal cells cannot be completely excluded. Taken together, our data demonstrate that functional restoration is obtained in adult mice when LRIT3 is localized at the OPL.

It became clear that using the PR-$Lrit3$ construct, a significantly better outcome was obtained, as 25% of mice injected with the PR-$Lrit3$ construct presented a strong scotopic ERG b-wave signal with significant restoration at the GC level upon MEA. Indeed, while the fraction of cells presenting ON-responses seems to increase using the

$Lrit3^{-/-}$-PR-$Lrit3$ condition, this is not the case for the other constructs, indicating a possible recruitment of more synapses with the expression of $Lrit3$ in photoreceptors. The amplitude of the rescue that we describe herein is greater than previously reported in age-matched mice,[22,23] likely due to the highly efficient vector and promoter combination used. Yet, an even greater signal might be obtained by using subretinal injection, which still seems to be the ideal route of administration to target photoreceptors.[20] Different reasons may account for the fact that restoration was only obtained in a significant number of animals when PR cells were targeted. One could be the predominant expression of $Lrit3$ in PRs, and thus targeting PRs re-establishes the normal pathway. However, our studies also showed partial restoration when ON-BCs were targeted, although in few animals. Delayed ON-responses at the level of RGCs were noted in these animals, which could potentially be due to the expression of LRIT3 in ON-BCs instead of PR where $Lrit3$ is probably naturally expressed, slowing down the process. However, the origin of these responses on the GC level is not fully understood since they could not be blocked by L-AP4. It may be a technical issue or of mechanistic origin. More treated mice with this construct would have been needed to make a real conclusion. The less efficient treatment with the BC-$Lrit3$ construct could also be explained by the fact that BCs are more difficult to target than PRs.[35] This is especially the case in mature retinas (only 6% of injected mice presented a b-wave versus 25% for the PR-$Lrit3$ construct) while some functional rescue has already been described following BC targeting in pups.[36] Again, since these observations were only noted in one animal, we cannot conclude on these hypotheses. In case of co-injection to target both ON-BCs and PRs, a stronger effectiveness was expected since both sides of the synaptic cleft were targeted; however, this was not the case. The effect of each construct might have been decreased by the co-injection, since each vector was diluted at 50% to have the same injection volume, compared to injection of only one construct.

Interestingly, function as measured by ERG and improved optomotor responses were only obtained under scotopic conditions, indicating that solely night vision was partially restored. In the study from

Scalabrino et al.[22] aiming to restore nyctalopin expression in ON-BCs, partial restoration of the scotopic b-wave was obtained while the restoration of the photopic response was less evident. Similarly, partial restoration under scotopic but not photopic conditions was reported in a study where *Lrit3* knockout mice were intravitreally injected with an AAV vector targeting rod PRs using a rhodopsin promoter.[23] The authors argued that this could be due to the fact that only rod but not cone PRs were targeted.[23] However, in our study with a GRK promoter, which targets rod and cone PRs, function under photopic condition was still not restored.

Secondary and possibly developmental effects might account for the lack of photopic restoration. Previously it was shown that cone synapses of $Lrit3^{-/-}$ mice have significantly less invaginating cone ON-BC dendrites compared to wild-type animals, indicating a role for LRIT3 in the development and or maintenance of the cone synapse.[17] Treatment of adult mice, where the synapse is fully formed, might not restore the cone-mediated pathway as the transmission between cones and cone ON-BCs is constitutively diminished. By performing electron microscopy after treatment, it would be interesting to follow up on the structure of the cone-to-cone BCs after treatment. However, as cones initiate ribbon synapse formation between P4 and P5 in mice,[37] and the cone synaptogenesis is completed by P14 to P15,[37,38] a restoration of the morphology of the cone synapses was not expected and was not studied. Furthermore, although our studies revealed LRIT3 restoration of protein localization in treated animals, the staining was more present in the OPL close to rods than cones explaining a functional rescue solely under scotopic conditions. In addition, it did not seem that TRPM1 localization at the dendritic tips of cone ON-BCs was restored conversely to rod BCs. These observations confirm the probable greater remodeling capacity of these synapses compared to cone-to-cone BCs synapses, even in adult mice, as previously discussed by Wang and coworkers.[39] This implication of CSNB proteins in synaptic development was also noticed in the $Grm6^{tm1Nak}$ mouse, in which invaginating dendrites of rod BCs are larger and often contain ectopic ribbons while the number of invaginating dendrites of cone ON-BCs and ribbons decrease at the cone pedicle, as observed in the $Lrit3^{-/-}$ mouse model.[17] Other molecules implicated in the development of the ribbon synapse might be influenced at an early developmental stage by the absence of LRIT3 and thus would explain the absence of rescue when treatment occurs at an adult stage. Treatment at a younger age using a promoter-targeting cone PRs and delivery of other molecules influenced by the absence of LRIT3 might rescue the photopic phenotype in $Lrit3^{-/-}$ mice. Furthermore, it would be interesting to measure the function of cones or cone-BCs with transgenic LRIT3 by patch-clamp recordings to see whether a functional rescue can be obtained, as previously described using a reporter gene.[22] However, as there might be an influence of the reporter gene on the conformation and/or interactions of LRIT3 and keeping in mind a future gene therapy approach for patients, we did not follow this approach.[40]

Of note, even though they are the most used animal models, the photopic phenotype of cCSNB mice models is in general more severe than the one of patients or larger animal models. Indeed, no b-wave is measured in photopic conditions in any of the cCSNB mouse models[2] while cone-driven responses are comparable between CNSB dogs, horses, and patients, e.g., mildly reduced;[2,41–43] scotopic ERG responses are similar in all models.[2] This difference of the cone ERG b-wave might be explained by the different cellular contribution that was noted between rodents and primates. For example, in the latter, OFF-BCs contribute to a large proportion of the photopic ERG b-wave responses[44] while in the mouse photopic ERG, only a small contribution of the OFF-BCs was noted.[45] Taken together, as different pathways could be implicated in the cone-driven responses in mice leading to a severer photopic phenotype and rendering a functional restoration under photopic conditions hardly achievable, mice models of CSNB might not be the ideal ones to assess cone-driven pathway restoration following treatment. The gene therapy approach described in this study should be further tested on larger animal models such as the CSNB beagle dog affected by *LRIT3* mutations[46] to more precisely evaluate the photopic phenotype. To conclude, this study reports a restoration of night vision in adult mice displaying congenital stationary night blindness as assessed by immunolocalization studies, ERG recordings, MEA analysis, and optomotor responses measurements due to the use of a specific vector and promoter combination.

MATERIALS AND METHODS
Ethical statement
All animal procedures were performed according to the Council Directive 2010/63EU of the European Parliament and the Council of September 22, 2010, on the protection of animals used for scientific purposes, with the National Institutes of Health guidelines and with the ARVO Statement for the Use of Animals in Ophthalmic and Vision Research. They were approved by the French Minister of National Education, Superior Education and Research (authorization delivered on January 21, 2019). When possible, all mice showing a restoration on ERG after treatment went through optomotor measurements, MEA, and immunolocalization studies.

AAV production
The production of recombinant AAVs was made by following the plasmid cotransfection method.[47] Lysates were then purified using iodixanol gradient ultracentrifugation as previously described: 40% iodixanol fraction was concentrated and buffer exchanged using Amicon Ultra-15 Centrifugal Filter Units (Merck Millipore, Billerica, MA, USA). Real-time PCR was used to titer the vector stocks for DNase-resistant vector genomes relatively to a standard.[48]

Intravitreal injections
Mice were anesthetized by isoflurane inhalation (5% in oxygen for induction and 2% for maintenance). Intravitreal injections in the right eyes were P30. Pupils were dilated (0.5% mydriaticum) and a 33-gauge needle was passed through the sclera at the ora serrata level. 1 μL of a viral stock solution at a concentration of 1.73 10^{14} vg/mL maximum was injected directly in the vitreous cavity. The left eyes were injected with PBS1X.

Immunolocalization studies

Animals were sacrificed by CO_2 inhalation followed by cervical dislocation. Eyes were removed and dissected to keep the posterior part of the eyes, which were then fixed in ice-cold 4% paraformaldehyde for 20 min. Subsequently, the eye cups were washed in ice-cold PBS and cryoprotected by increasing concentrations of sucrose (ranging from 10% to 30%) in water and 0.12 M phosphate buffer for 1 h at 4°C for 10% sucrose and 20% sucrose solutions and overnight at 4°C under agitation for the 30% sucrose solution. The eye cups were then embedded in 7.5% gelatin and 10% sucrose, and the blocks were frozen at −40°C in isopentane and kept at −80°C until cutting. Sections of 12 μm were generated using a cryostat (MICROM HM 560, Thermo-Fisher Scientific, Waltham, MA, USA) and mounted on glass slides (Superfrost Plus, ThermoFisher Scientific). Mouse retina sections were treated to decrease background noise (Antigen Retrieval Reagent, Biotechne, Minneapolis, MN, USA) for 4 min at 92°C and subsequently blocked for 1 h at room temperature in PBS1X 10% Donkey Serum (v/v), 0.1% Triton X-100. Primary antibodies and the dilutions used were as follows: rabbit anti-LRIT3 (1:200, Neuillé et al., 2015), guinea pig anti-mGluR6 (1:15,000, AP20134SUN, Acris, Herford, Germany), rabbit cone-arrestin (1:2,000, ab15282, Abcam, Cambridge, UK), mouse anti-PKCα (1:1,000, P5704 Sigma-Aldrich, Darmstadt, Germany), lectin PNA 594 conjugate (1:1,000, L32459, Life Technologies, Grand Island, NY, USA), and sheep anti-TRPM1 (1:500).[49] The sections were incubated with primary antibodies diluted in PBS1X 2% Donkey Serum (v/v) and 0.1% Triton X-100 for 1 h at room temperature. After washes with PBS1X 0.1% Triton X-100, the sections were incubated with anti-rabbit and anti-sheep secondary antibodies coupled with Alexa Fluor 488, or Cy3 (Jackson ImmunoResearch) along with 4',6-diamidino-2-phenylindole (DAPI), all used at 1:1,000, for 0.5 h at room temperature. Subsequently, the sections were coverslipped with mounting medium (Mowiol, Merck Millipore, Billerica, MA, USA). Fluorescence images retinal sections were acquired with a confocal microscope (FV1000, Olympus). Images for figures were handled with the ImageJ software (ImageJ Software).

Electroretinogram

Mice were DA overnight before performing the ERG recordings. They were anesthetized by ketamine (80 mg/kg) and xylazine (8 mg/kg) and eye drops were used to dilate their pupils (0.5% mydriaticum 5% neosynephrine) and anesthetize the cornea (0.4% oxybuprocaine chlorohydrate). Mice corporal temperature was maintained through a heating pad along the test. Upper and lower eyelids were retracted to keep the eyes opened and bulging. Corneal lenses (Mayo Corporation, Japan) were applied on corneal surface to record the ERG. A reference electrode was placed on the nose while the ground electrode was placed above the tail. Recordings from both eyes were made in parallel to compare infected to non-infected eyes. All scotopic ERG were made first using six increasing light intensity of flashes ranging from 0.003 to 30.0 cd. s/m². Each trace corresponding to one light intensity results from the average of five traces originating from five flashes. To ensure a saturation of rod PRs and the recording of cone-driven responses, we performed a 10-min light-adaptation step at 20 cd/m². Following this light-adaptation step, photopic ERGs were recorded first at 3.0 cd. s/

m² and at the same intensity; 5 Hz and 10 Hz flickers were also checked. All data were analyzed with GraphPad Prism v.6 (GraphPad Software, La Jolla, CA, USA). The b-wave amplitude was manually calculated from the peak of the a-wave to the peak of the b-wave.

MEA

After overnight dark adaptation, mice were sacrificed by CO_2 inhalation followed by cervical dislocation. Retinas were carefully dissected under dim red light and conserved in Ames medium (Sigma-Aldrich, St. Louis, MO, USA) oxygenated with 95% oxygen and 5% CO_2. Retinas were placed on a Spectra/Por membrane (Spectrum Laboratories, Rancho Dominguez, CA, USA) previously coated with poly-D-lysine and gently pressed against an MEA (MEA256 100/30 iR-ITO; Multi Channel Systems MCS, Reutlingen, Germany) using a micromanipulator, with RGCs facing the electrodes. Retinas were continuously perfused with bubbled Ames medium at 34°C at a rate of 1 to 2 mL/min and left to rest for 45 min before the recording session. Under dark conditions, 10 repeated full-field light stimuli at a 450 nm wavelength were applied to the samples at 4.10^{11} photons/cm²/s for 2 s with 10 s interval by using a Polychrome V monochromator (Olympus, Hamburg, Germany) driven by an STG2008 stimulus generator (MCS). Raw RGC activity recorded by MEA was amplified (gain 1,000–1,200) and sampled at 20 kHz by using MCRack software (MCS). The resulting data were stored and filtered with a 200-Hz high-pass filter. Raster plots were obtained by using a combination of threshold detection, template matching, and cluster grouping based on principal component analysis using Spike2 v.7 software (CED, Cambridge, UK). Peristimulus time histograms were plotted with a bin size of 50 ms by using a custom-made script in MATLAB v.R2014b (MathWorks, Natick, MA, USA). Only RGCs with a mean spontaneous firing frequency superior to 1 Hz were considered. We subsequently determined for each sorted RGC the maximum firing frequency in an interval of 2 s after light onset (for ON-responses) and in an interval of 2 s after light offset (for OFF-responses). These values were adjusted to the mean spontaneous firing frequency of the corresponding RGC. Considering that significant responses have a maximum firing frequency that is superior to the mean spontaneous firing frequency þ 5 SD, we determined the time at which these significant frequencies were reached after the light onset for ON-responses and after the light offset for OFF-responses. The histograms were traced with GraphPad Prism v.6 (GraphPad Software, La Jolla, CA, USA). Detailed description on experiments with bath application of the mGluR6 agonist L-AP4 will be provided upon request.

Optomotor test

Optomotor test was performed as described previously.[16] Mice were DA overnight before the optomotor test. Eight wild-type animals and eight knockout animals of each lineage were studied along with the treated animals (PR-*Lrit3* n = 4, BC-*Lrit3* n = 2, OPL-*Lrit3* n = 1). Mice were placed on a grid platform (11.5 cm diameter, 19 cm above the bottom of the drum) at the center of a motorized drum (29 cm diameter) covered by vertical black and white stripes of a defined spatial frequency (0.063, 0.125, 0.25, 0.5, and 0.75 cycles per degree). A 5 min break was made before the test so the animal could get used to its new environment. The stripes were rotated for 1 min clockwise

and 1 min counterclockwise at a speed of 2 rotations per min. An interval of 10 s was made after the first min. Each test was recorded with a digital infrared camera to count head movements of the mice. Tests were first performed under scotopic conditions and then in photopic condition after 5 min of light adaptation (two lamps of 60 Watts). Head movements in both directions were considered to obtain the number of head movements per minute.

Statistical analysis

Mann-Whitney statistical analysis was performed for the scotopic ERG b-wave persistence and optomotor responses significance evaluation. We chose an unpaired t test and non-parametric test because the groups were not related and a Gaussian distribution of the data with the small number of animals involved was not expected. The star indicates a significant test ($p < 0.05$; Figure 5).

SUPPLEMENTAL INFORMATION

Supplemental information can be found online at https://doi.org/10.1016/j.omtm.2021.05.008.

ACKNOWLEDGMENTS

AUTHOR CONTRIBUTIONS

J.V. wrote the manuscript; G.G. wrote the MEA part of the manuscript; J.V., N.B., C.J., M.D., C.R., M.M.D.S.D., M. Neuillé, and C.M. performed the experiments; J.V. and G.G. (MEA) analyzed the results; J.-A.S., S.P., and D.D. co-supervised the study; M. Nassisi, I.A., and D.D. gave their input in the study design and manuscript writing; C.Z. designed the study, supervised the experiments, and corrected the manuscript writing.

DECLARATION OF INTERESTS

The funders had no role in study design, data collection, analysis and interpretation, decision to publish, or preparation of the manuscript. J.V., D.D., S.P., I.A., J.-A.S., and C.Z. are inventors on a pending patent application on "Treatment of congenital stationary night blindness using gene therapy" (SL0160 [CLBEnaco-F2478 36WO]). D.D. is an inventor on a patent of adeno-associated virus virions with variant capsid and methods of use thereof with royalties paid to Avalanche Biotech (WO2012145601 A2).

REFERENCES

1. Zeitz, C., Robson, A.G., and Audo, I. (2015). Congenital stationary night blindness: an analysis and update of genotype-phenotype correlations and pathogenic mechanisms. Prog. Retin. Eye Res. 45, 58–110.

2. Schubert, G., and Bornschein, H. (1952). [Analysis of the human electroretinogram]. Ophthalmologica 123, 396–413.

3. Miyake, Y., Yagasaki, K., Horiguchi, M., Kawase, Y., and Kanda, T. (1986). Congenital stationary night blindness with negative electroretinogram. A new classification. Arch. Ophthalmol. 104, 1013–1020.

4. Miyake, Y., Yagasaki, K., Horiguchi, M., and Kawase, Y. (1987). On- and off-responses in photopic electroretinogram in complete and incomplete types of congenital stationary night blindness. Jpn. J. Ophthalmol. 31, 81–87.

5. Pusch, C.M., Zeitz, C., Brandau, O., Pesch, K., Achatz, H., Feil, S., Scharfe, C., Maurer, J., Jacobi, F.K., Pinckers, A., et al. (2000). The complete form of X-linked congenital stationary night blindness is caused by mutations in a gene encoding a leucine-rich repeat protein. Nat. Genet. 26, 324–327.

6. Bech-Hansen, N.T., Naylor, M.J., Maybaum, T.A., Sparkes, R.L., Koop, B., Birch, D.G., Bergen, A.A., Prinsen, C.F., Polomeno, R.C., Gal, A., et al. (2000). Mutations in NYX, encoding the leucine-rich proteoglycan nyctalopin, cause X-linked complete congenital stationary night blindness. Nat. Genet. 26, 319–323.

7. Audo, I., Kohl, S., Leroy, B.P., Munier, F.L., Guillonneau, X., Mohand-Saïd, S., Bujakowska, K., Nandrot, E.F., Lorenz, B., Preising, M., et al. (2009). TRPM1 is mutated in patients with autosomal-recessive complete congenital stationary night blindness. Am. J. Hum. Genet. 85, 720–729.

8. Li, Z., Sergouniotis, P.I., Michaelides, M., Mackay, D.S., Wright, G.A., Devery, S., Moore, A.T., Holder, G.E., Robson, A.G., and Webster, A.R. (2009). Recessive mutations of the gene TRPM1 abrogate ON bipolar cell function and cause complete congenital stationary night blindness in humans. Am. J. Hum. Genet. 85, 711–719.

9. van Genderen, M.M., Bijveld, M.M., Claassen, Y.B., Florijn, R.J., Pearring, J.N., Meire, F.M., McCall, M.A., Riemslag, F.C., Gregg, R.G., Bergen, A.A., and Kamermans, M. (2009). Mutations in TRPM1 are a common cause of complete congenital stationary night blindness. Am. J. Hum. Genet. 85, 730–736.

10. Zeitz, C., van Genderen, M., Neidhardt, J., Luhmann, U.F., Hoeben, F., Forster, U., Wycisk, K., Mátyás, G., Hoyng, C.B., Riemslag, F., et al. (2005). Mutations in GRM6 cause autosomal recessive congenital stationary night blindness with a distinctive scotopic 15-Hz flicker electroretinogram. Invest. Ophthalmol. Vis. Sci. 46, 4328–4335.

11. Dryja, T.P., McGee, T.L., Berson, E.L., Fishman, G.A., Sandberg, M.A., Alexander, K.R., Derlacki, D.J., and Rajagopalan, A.S. (2005). Night blindness and abnormal cone electroretinogram ON responses in patients with mutations in the GRM6 gene encoding mGluR6. Proc. Natl. Acad. Sci. USA 102, 4884–4889.

12. Audo, I., Bujakowska, K., Orhan, E., Poloschek, C.M., Defoort-Dhellemmes, S., Drumare, I., Kohl, S., Luu, T.D., Lecompte, O., Zrenner, E., et al. (2012). Whole-exome sequencing identifies mutations in GPR179 leading to autosomal-recessive complete congenital stationary night blindness. Am. J. Hum. Genet. 90, 321–330.

13. Peachey, N.S., Ray, T.A., Florijn, R., Rowe, L.B., Sjoerdsma, T., Contreras-Alcantara, S., Baba, K., Tosini, G., Pozdeyev, N., Iuvone, P.M., et al. (2012). GPR179 is required for depolarizing bipolar cell function and is mutated in autosomal-recessive complete congenital stationary night blindness. Am. J. Hum. Genet. 90, 331–339.

14. Zeitz, C., Jacobson, S.G., Hamel, C.P., Bujakowska, K., Neuillé, M., Orhan, E., Zanlonghi, X., Lancelot, M.E., Michiels, C., Schwartz, S.B., et al.; Congenital Stationary Night Blindness Consortium (2013). Whole-exome sequencing identifies LRIT3 mutations as a cause of autosomal-recessive complete congenital stationary night blindness. Am. J. Hum. Genet. 92, 67–75.

15. Pardue, M.T., and Peachey, N.S. (2014). Mouse b-wave mutants. Doc. Ophthalmol. *128*, 77–89.

16. Neuillé, M., El Shamieh, S., Orhan, E., Michiels, C., Antonio, A., Lancelot, M.E., Condroyer, C., Bujakowska, K., Poch, O., Sahel, J.A., et al. (2014). Lrit3 deficient mouse (nob6): a novel model of complete congenital stationary night blindness (cCSNB). PLoS ONE *9*, e90342.

17. Neuillé, M., Cao, Y., Caplette, R., Guerrero-Given, D., Thomas, C., Kamasawa, N., Sahel, J.A., Hamel, C.P., Audo, I., Picaud, S., et al. (2017). LRIT3 Differentially Affects Connectivity and Synaptic Transmission of Cones to ON- and OFF-Bipolar Cells. Invest. Ophthalmol. Vis. Sci. *58*, 1768–1778.

18. Neuillé, M., Morgans, C.W., Cao, Y., Orhan, E., Michiels, C., Sahel, J.A., Audo, I., Duvoisin, R.M., Martemyanov, K.A., and Zeitz, C. (2015). LRIT3 is essential to localize TRPM1 to the dendritic tips of depolarizing bipolar cells and may play a role in cone synapse formation. Eur. J. Neurosci. *42*, 1966–1975.

19. Hasan, N., Pangeni, G., Ray, T.A., Fransen, K.M., Noel, J., Borghuis, B.G., McCall, M.A., and Gregg, R.G. (2020). LRIT3 is required for Nyctalopin expression and normal ON and OFF pathway signaling in the retina. eNeuro *7*, ENEURO.0002-20.2020.

20. Trapani, I., and Auricchio, A. (2018). Seeing the Light after 25 Years of Retinal Gene Therapy. Trends Mol. Med. *24*, 669–681.

21. Mace, E., Caplette, R., Marre, O., Sengupta, A., Chaffiol, A., Barbe, P., Desrosiers, M., Bamberg, E., Sahel, J.A., Picaud, S., et al. (2015). Targeting channelrhodopsin-2 to ON-bipolar cells with vitreally administered AAV Restores ON and OFF visual responses in blind mice. Mol. Ther. *23*, 7–16.

22. Scalabrino, M.L., Boye, S.L., Fransen, K.M., Noel, J.M., Dyka, F.M., Min, S.H., Ruan, Q., De Leeuw, C.N., Simpson, E.M., Gregg, R.G., et al. (2015). Intravitreal delivery of a novel AAV vector targets ON bipolar cells and restores visual function in a mouse model of complete congenital stationary night blindness. Hum. Mol. Genet. *24*, 6229–6239.

23. Hasan, N., Pangeni, G., Cobb, C.A., Ray, T.A., Nettesheim, E.R., Ertel, K.J., Lipinski, D.M., McCall, M.A., and Gregg, R.G. (2019). Presynaptic Expression of LRIT3 Transsynaptically Organizes the Postsynaptic Glutamate Signaling Complex Containing TRPM1. Cell Rep. *27*, 3107–3116.e3.

24. Varin, J., Bouzidi, N., Dias, M.M.S., Pugliese, T., Michiels, C., Robert, C., Desrosiers, M., Sahel, J.A., Audo, I., Dalkara, D., and Zeitz, C. (2021). Restoration of mGluR6 Localization Following AAV-Mediated Delivery in a Mouse Model of Congenital Stationary Night Blindness. Invest. Ophthalmol. Vis. Sci. *62*, 24.

25. Khani, S.C., Pawlyk, B.S., Bulgakov, O.V., Kasperek, E., Young, J.E., Adamian, M., Sun, X., Smith, A.J., Ali, R.R., and Li, T. (2007). AAV-mediated expression targeting of rod and cone photoreceptors with a human rhodopsin kinase promoter. Invest. Ophthalmol. Vis. Sci. *48*, 3954–3961.

26. Dalkara, D., Byrne, L.C., Klimczak, R.R., Visel, M., Yin, L., Merigan, W.H., Flannery, J.G., and Schaffer, D.V. (2013). In vivo-directed evolution of a new adeno-associated virus for therapeutic outer retinal gene delivery from the vitreous. Sci. Transl. Med. *5*, 189ra76.

27. Abdeljalil, J., Hamid, M., Abdel-Mouttalib, O., Stéphane, R., Raymond, R., Johan, A., José, S., Pierre, C., and Serge, P. (2005). The optomotor response: a robust first-line visual screening method for mice. Vision Res. *45*, 1439–1446.

28. Leber, T. (1869). Uber retinitis pigmentosa und angeborene amaurose. Graefe's archive for clinical and experimental ophthalmology =. Albrecht Von Graefes Arch. Klin. Exp. Ophthalmol. *15*, 1–25.

29. Marlhens, F., Bareil, C., Griffoin, J.M., Zrenner, E., Amalric, P., Eliaou, C., Liu, S.Y., Harris, E., Redmond, T.M., Arnaud, B., et al. (1997). Mutations in RPE65 cause Leber's congenital amaurosis. Nat. Genet. *17*, 139–141.

30. Bainbridge, J.W., Smith, A.J., Barker, S.S., Robbie, S., Henderson, R., Balaggan, K., Viswanathan, A., Holder, G.E., Stockman, A., Tyler, N., et al. (2008). Effect of gene therapy on visual function in Leber's congenital amaurosis. N. Engl. J. Med. *358*, 2231–2239.

31. Cideciyan, A.V., Aleman, T.S., Boye, S.L., Schwartz, S.B., Kaushal, S., Roman, A.J., Pang, J.J., Sumaroka, A., Windsor, E.A., Wilson, J.M., et al. (2008). Human gene therapy for RPE65 isomerase deficiency activates the retinoid cycle of vision but with slow rod kinetics. Proc. Natl. Acad. Sci. USA *105*, 15112–15117.

32. Maguire, A.M., Simonelli, F., Pierce, E.A., Pugh, E.N., Jr., Mingozzi, F., Bennicelli, J., Banfi, S., Marshall, K.A., Testa, F., Surace, E.M., et al. (2008). Safety and efficacy of gene transfer for Leber's congenital amaurosis. N. Engl. J. Med. *358*, 2240–2248.

33. Shekhar, K., Lapan, S.W., Whitney, I.E., Tran, N.M., Macosko, E.Z., Kowalczyk, M., Adiconis, X., Levin, J.Z., Nemesh, J., Goldman, M., et al. (2016). Comprehensive Classification of Retinal Bipolar Neurons by Single-Cell Transcriptomics. Cell *166*, 1308–1323.e30.

34. Miyadera, K., Roszak, K., Ripolles Garcia, A., Santana, E., Iffrig, S.M., Visel, M., Byrne, L., Beltran, W.A., Flannery, J.G., and Aguirre, G.D. (2020). AAV gene therapy restores ON-bipolar cell function in a canine model of LRIT3-congenital stationary night blindness. Invest. Ophthalmol. Vis. Sci. *61*, 2298, 2298.

35. van Wyk, M., Hulliger, E.C., Girod, L., Ebneter, A., and Kleinlogel, S. (2017). Present Molecular Limitations of ON-Bipolar Cell Targeted Gene Therapy. Front. Neurosci. *11*, 161.

36. Kleine Holthaus, S.M., Aristorena, M., Maswood, R., Semenyuk, O., Hoke, J., Hare, A., Smith, A.J., Mole, S.E., and Ali, R.R. (2020). Gene Therapy Targeting the Inner Retina Rescues the Retinal Phenotype in a Mouse Model of CLN3 Batten Disease. Hum. Gene Ther. *31*, 709–718.

37. Sherry, D.M., Wang, M.M., Bates, J., and Frishman, L.J. (2003). Expression of vesicular glutamate transporter 1 in the mouse retina reveals temporal ordering in development of rod vs. cone and ON vs. OFF circuits. J. Comp. Neurol. *465*, 480–498.

38. Rich, K.A., Zhan, Y., and Blanks, J.C. (1997). Migration and synaptogenesis of cone photoreceptors in the developing mouse retina. J. Comp. Neurol. *388*, 47–63.

39. Wang, T., Pahlberg, J., Cafaro, J., Frederiksen, R., Cooper, A.J., Sampath, A.P., Field, G.D., and Chen, J. (2019). Activation of Rod Input in a Model of Retinal Degeneration Reverses Retinal Remodeling and Induces Formation of Functional Synapses and Recovery of Visual Signaling in the Adult Retina. J. Neurosci. *39*, 6798–6810.

40. Stadler, C., Rexhepaj, E., Singan, V.R., Murphy, R.F., Pepperkok, R., Uhlén, M., Simpson, J.C., and Lundberg, E. (2013). Immunofluorescence and fluorescent-protein tagging show high correlation for protein localization in mammalian cells. Nat. Methods *10*, 315–323.

41. Kondo, M., Das, G., Imai, R., Santana, E., Nakashita, T., Imawaka, M., Ueda, K., Ohtsuka, H., Sakai, K., Aihara, T., et al. (2015). A Naturally Occurring Canine Model of Autosomal Recessive Congenital Stationary Night Blindness. PLoS ONE *10*, e0137072.

42. Witzel, D.A., Smith, E.L., Wilson, R.D., and Aguirre, G.D. (1978). Congenital stationary night blindness: an animal model. Invest. Ophthalmol. Vis. Sci. *17*, 788–795.

43. Sandmeyer, L.S., Breaux, C.B., Archer, S., and Grahn, B.H. (2007). Clinical and electroretinographic characteristics of congenital stationary night blindness in the Appaloosa and the association with the leopard complex. Vet. Ophthalmol. *10*, 368–375.

44. Sieving, P.A., Murayama, K., and Naarendorp, F. (1994). Push-pull model of the primate photopic electroretinogram: a role for hyperpolarizing neurons in shaping the b-wave. Vis. Neurosci. *11*, 519–532.

45. Sharma, S., Ball, S.L., and Peachey, N.S. (2005). Pharmacological studies of the mouse cone electroretinogram. Vis. Neurosci. *22*, 631–636.

46. Das, R.G., Becker, D., Jagannathan, V., Goldstein, O., Santana, E., Carlin, K., Sudharsan, R., Leeb, T., Nishizawa, Y., Kondo, M., et al. (2019). Genome-wide association study and whole-genome sequencing identify a deletion in LRIT3 associated with canine congenital stationary night blindness. Sci. Rep. *9*, 14166.

47. Choi, V.W., Asokan, A., Haberman, R.A., and Samulski, R.J. (2007). Production of recombinant adeno-associated viral vectors for in vitro and in vivo use. Curr. Protoc. Mol. Bio. Chapter 16, Unit 16 25.

48. Aurnhammer, C., Haase, M., Muether, N., Hausl, M., Rauschhuber, C., Huber, I., Nitschko, H., Busch, U., Sing, A., Ehrhardt, A., and Baiker, A. (2012). Universal real-time PCR for the detection and quantification of adeno-associated virus serotype 2-derived inverted terminal repeat sequences. Hum. Gene Ther. Methods *23*, 18–28.

49. Cao, Y., Posokhova, E., and Martemyanov, K.A. (2011). TRPM1 forms complexes with nyctalopin in vivo and accumulates in postsynaptic compartment of ON-bipolar neurons in mGluR6-dependent manner. J Neurosci *31*, 11521–11526.